Exact Displacement Analysis of Four-Link Spatial Mechanisms by the Direction Cosine Matrix Method

T. C. Huang
Professor,
Department of Engineering Mechanics,
University of Wisconsin,
Madison, Wisc. 53706
Mem. ASME

Y. Youm
Associate Professor,
Department of Mechanical Engineering,
Catholic University of America,
Washington, D.C.
Mem. ASME

A method of displacement analysis of the four-link spatial mechanism is developed. The results through this analysis will be exact solutions that can be obtained without resorting to numerical or iteration schemes. In the analysis, the position of a link in a mechanism can be fully defined if its direction and length are known. Therefore, this analysis involves the calculation of the unknown direction cosines and length of each link for a given configuration of the mechanism. In finding the direction cosines of the unknown unit vectors involved for each link and rotating axis, two types of coordinates, the global and the local, are generally used. Then, a direction cosine matrix between each local coordinate system and the global coordinates is established. Thus, the unknown direction cosines of the local coordinates, the links, and the rotating axes are obtained in global coordinates. In this development, direction cosine matrices are used throughout the analysis. As an illustration, the application of this method to the study of four-link spatial mechanisms, RGGR, RGCR, RRGG, and RRGC will be presented.

Introduction

A recent survey of space mechanism research [1], which covers analytical methods developed mainly since the 1950s with numerous pertinent references, serves as an extensive and informative source of background material. However, several selective references of well-known methods for the displacement analysis of spatial linkage may be mentioned. Among them are the 4×4 matrix iterative method [2, 3], the dual number quarternion method [4, 5], the geometric transformation method [6, 7], the vector method [8–10], the screw method [11–15], the tensor method [16], the line geometric method [17], and the geometrical configuration method [18], etc. Most of these methods involve high level mathematics of complicated mathematical manipulation, and all require numerical or iterative schemes for solutions.

A method of displacement analysis using direction cosine matrices as transformation matrices for the four-link spatial mechanisms is developed and applied to various four-bar spatial linkages in this paper. The mathematics involved are elementary; the operations are simple without loss of geometric interpretation, and the solutions are exact. The analysis starts by choosing an appropriate local coordinate system and assigns direction cosines to the related unit vectors. These direction cosines in the local coordinates are obtained by applying the dot product of unit vectors and using given angle data. Then, a direction cosine matrix between the global and the local coordinates is obtained, by using known unit vectors, the direction cosines of the local coordinates, and a special property of the direction cosine matrix. Using this special property of the direction cosine matrix, that is, that each element of the matrix equals its own cofactor, we obtain exact analytical solutions without resorting to numerical or iterative schemes. When the direction cosine matrix is known, the unknown unit vectors in the global coordinates can be fully calculated.

Analytical solutions in closed-form, input-output relations for a few spatial four-bar linkages are obtained in [4, 6, 7]. In [6, 7], the rotation matrix is used, together with one or two constraints particular to the linkage concerned. However, the solutions for these closed-form, input-output relations will have to be obtained by numerically solving transcendental equations. In the present paper, the direction cosine matrices are used in successive steps of the analysis, from the input end to the output end of the linkage mechanism. In the process, the constraints of the mechanism, such as the constant length of a link or the constant angle between two links, are taken care of automatically. The solutions are obtained without resorting to numerical or iteration schemes. It should be mentioned that, for a simple case of the 2R-2G mechanism, the input-output relation, developed in [20], can be reduced to a closed-form solution.

Contributed by the Applied Mechanics Division and presented at the Winter Annual Meeting, New Orleans, La., December 9–14, 1984 of THE AMERICAN SOCIETY OF MECHANICAL ENGINEERS.

Discussion on this paper should be addressed to the Editorial Department, ASME, United Engineering Center, 345 East 47th Street, New York, N.Y. 10017, and will be accepted until two months after final publication of the paper itself in the JOURNAL OF APPLIED MECHANICS. Manuscript received by ASME Applied Mechanics Division, December, 1982; final revision, July, 1984. Paper No. 84-WA/APM-22.

Copies will be available until August, 1985.

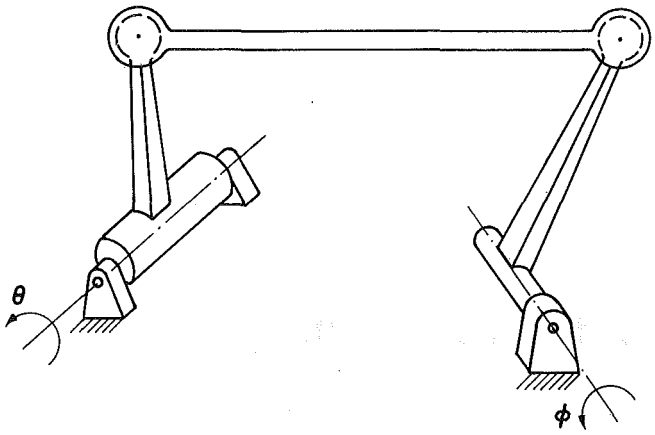

Fig. 1 A RGGR four-link spatial mechanism

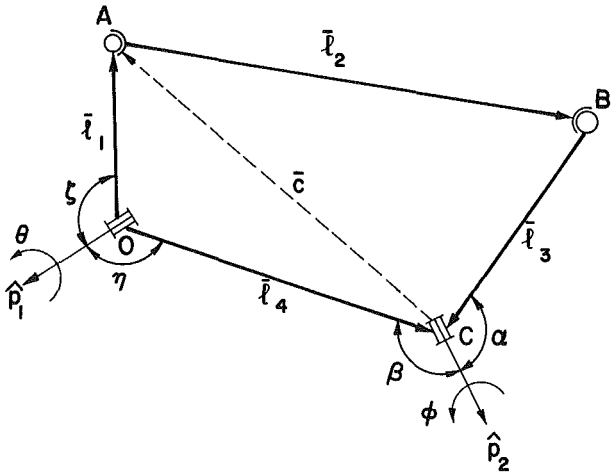

Fig. 2 The schematic diagram of a RGGR mechanism

In this paper, this direction cosine matrix method will be applied to obtain analytical solutions for the four-bar spatial linkages, an RGGR, an RGCR, an RRGG, and an RRGC, with numerical illustration.

1 Displacement Analysis of the RGGR Mechanism

The RGGR four-link spatial mechanism as shown in Fig. 1 is a generalization of the planar four-bar mechanism RRRR. It is one of the most versatile and practical configurations of three-dimensional mechanisms and will function as a single degree of freedom linkage with a passive degree of freedom in the connecting link. A schematic diagram of an RGGR mechanism is shown in Fig. 2.

The known quantities of the mechanism are the lengths, l_1, l_2, l_3, l_4, the vector $\bar{l}_4$, the directions of rotations, $\hat{p}_1$, $\hat{p}_2$, the angles ζ, η, α, β, from the construction of mechanism, and the input angle θ. The unknown quantities are $\hat{l}_1$, $\hat{l}_2$, and $\hat{l}_3$.

(a) Input Angle θ. The input angle θ for the rotation about the $\hat{p}_1$-axis can be measured with any arbitrary reference. As shown in Fig. 3, θ is chosen as the angle between the two planes formed by $\hat{p}_1$ and $\hat{l}_4$, and $\hat{p}_1$ and $\hat{l}_1$ in which the $\hat{p}_1\hat{l}_4$-plane chosen as a reference. Both the angle ζ between $\hat{p}_1$ and $\hat{l}_1$, and the angle η between $\hat{p}_1$ and $\hat{l}_4$ are chosen to be less than π.

Let the local coordinates x_1, y_1, z_1 associated with $\hat{p}_1$ with the origin at 0 be chosen as follows:

The x_1-axis is set along the known rotating axis $\hat{p}_1$ and has the same positive direction as $\hat{p}_1$.

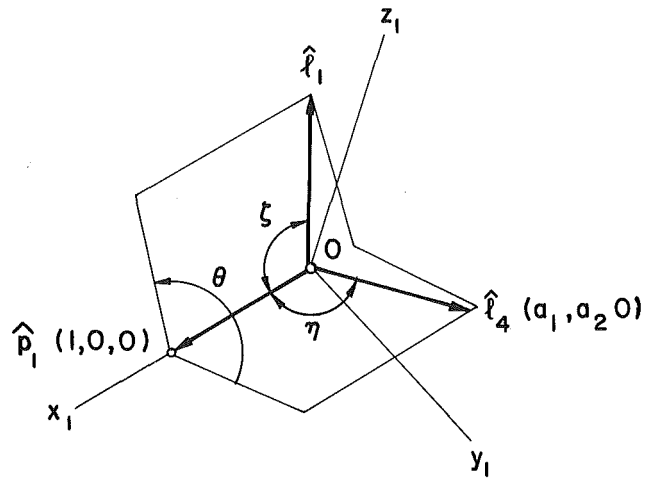

Fig. 3 A local coordinate system and input angle measurement

The y_1-axis is set in the plane of $\hat{p}_1$ and $\hat{l}_4$ and the angle between $\hat{l}_4$ and the y-axis is less than $\pi/2$.

The z_1-axis follows the right-hand rule.

With this local coordinate system the input angle θ can now be measured between the x_1y_1-plane and the x_1l_1-plane with the x_1y_1-plane as references.

(b) Analysis of $\hat{l}_1$. The direction cosines of the unit vectors $\hat{p}_1$, $\hat{l}_1$, and $\hat{l}_4$ in the local coordinates system associated with $\hat{p}_1$ are expressed in the parenthesis for each unit vector as $\hat{p}_1(1, 0, 0)$, $\hat{l}_1$ $(\cos\zeta, \sin\zeta\cos\theta, \sin\zeta\sin\theta)$, and $\hat{l}_4(a_1', a_2', 0)$, respectively.

To find $\hat{l}_1$ in global coordinates, the direction cosine transformation matrix $[T_{ij}]$ should be defined. With $\hat{p}_1$ and $\hat{l}_4$ known in global coordinates we have

$$\{\hat{p}_{1x},\hat{p}_{1y},\hat{p}_{1z}\}^T_{\text{global}} = [T_{ij}]_1 \underset{L\to G}{} \{1,0,0\}^T_{\text{local}} \tag{1}$$

from which

$$(T_{11})_1 = \hat{p}_{1x}, \quad (T_{21})_1 = \hat{p}_{1y}, \quad (T_{31})_1 = \hat{p}_{1z} \tag{2}$$

$L\to G$ underneath $[T_{ij}]_1$ indicates transformation from local to global coordinates. From now on the subscripts global, local, and $L\to G$ will be omitted for simplicity. Similarly,

$$\{\hat{l}_{4x},\hat{l}_{4y},\hat{l}_{4z}\}^T = [T_{ij}]_1\{a_1',a_2',0\}^T \tag{3}$$

in which

$$a_1' = \hat{l}_4 \cdot \hat{p}_1 = \cos\eta \tag{4}$$

$$a_2' = \sqrt{1-(a_1')^2} = \sin\eta \tag{5}$$

where positive sign is taken for the square root as a result of construction of the local coordinate system. Thus

$$\{\hat{l}_{4x},\hat{l}_{4y},\hat{l}_{4z}\}^T = [T_{ij}]_1\{\cos\eta,\sin\eta,0\}^T \tag{6}$$

or

$$\begin{aligned}
\hat{l}_{4x} &= (T_{11})_1\cos\eta + (T_{12})_1\sin\eta \\
\hat{l}_{4y} &= (T_{21})_1\cos\eta + (T_{22})_1\sin\eta \\
\hat{l}_{4z} &= (T_{31})_1\cos\eta + (T_{32})_1\sin\eta
\end{aligned} \tag{7}$$

Solving $(T_{12})_1$, $(T_{22})_1$, and $(T_{32})_1$ gives

$$\begin{aligned}
(T_{12})_1 &= (\hat{l}_{4x} - \hat{p}_{1x}\cos\eta)/\sin\eta \\
(T_{22})_1 &= (\hat{l}_{4y} - \hat{p}_{1y}\cos\eta)/\sin\eta \\
(T_{32})_1 &= (\hat{l}_{4z} - \hat{p}_{1z}\cos\eta)/\sin\eta
\end{aligned} \tag{8}$$

Now $(T_{13})_1$, $(T_{23})_1$, and $(T_{33})_1$ can be found as their cofactors. Thus

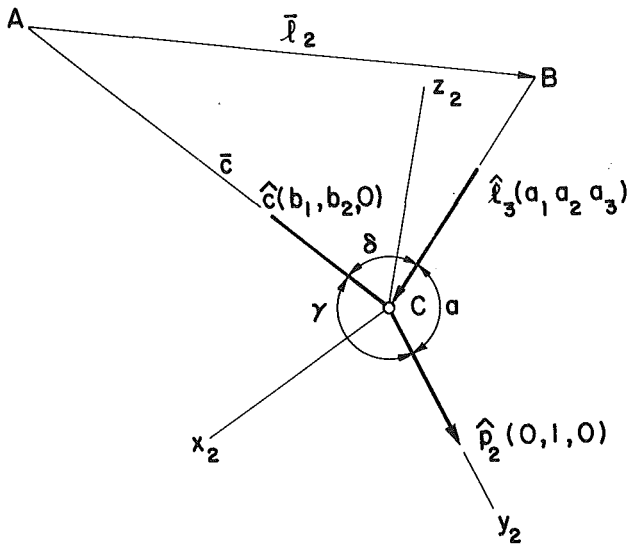

Fig. 4 A local coordinate system and links l_2 and l_3

$$(T_{13})_1 = (\hat{p}_{1y}\hat{l}_{4z} - \hat{p}_{1z}\hat{l}_{4y})/\sin\eta$$
$$(T_{23})_1 = -(\hat{p}_{1x}\hat{l}_{4z} - \hat{p}_{1z}\hat{l}_{4x})/\sin\eta$$
$$(T_{33})_1 = (\hat{p}_{1x}\hat{l}_{4y} - \hat{p}_{1y}\hat{l}_{4x})/\sin\eta \tag{9}$$

Therefore

$$[T_{ij}]_1 = \frac{1}{\sin\eta}\begin{bmatrix} \hat{p}_{1x}\sin\eta & \hat{l}_{4x} - \hat{p}_{1x}\cos\eta & \hat{p}_{1y}\hat{l}_{4z} - \hat{p}_{1z}\hat{l}_{4y} \\ \hat{p}_{1y}\sin\eta & \hat{l}_{4y} - \hat{p}_{1y}\cos\eta & \hat{p}_{1z}\hat{l}_{4x} - \hat{p}_{1x}\hat{l}_{4z} \\ \hat{p}_{1z}\sin\eta & \hat{l}_{4z} - \hat{p}_{1z}\cos\eta & \hat{p}_{1x}\hat{l}_{4y} - \hat{p}_{1y}\hat{l}_{4x} \end{bmatrix} \tag{10}$$

Now $\hat{l}_1$ in global coordinates can be found as

$$\{\hat{l}_{1x}, \hat{l}_{1y}, \hat{l}_{1z}\}^T = [T_{ij}]_1 \{\cos\zeta,\ \sin\zeta\cos\theta,\ \sin\zeta\sin\theta\}^T \tag{11}$$

(c) Analysis of $\hat{l}_3$. Let vector $\bar{c}$ be defined such that it forms a closed loop with vectors $\bar{l}_2$ and $\bar{l}_3$ as shown in Fig. 4. It also forms a closed loop with vectors $\bar{l}_1$ and $\bar{l}_4$. From the figure

$$\bar{c} = \bar{l}_1 - \bar{l}_4 \quad \text{and} \quad \hat{c} = \bar{c}/|\bar{c}| \tag{12}$$

A local coordinate system with the origin at joint C is set such that the y_2-axis is along the known vector $\hat{p}_2$ as shown in Fig. 4. The x_2-axis is in the plane that consists of known vectors $\bar{c}$ and $\hat{p}_2$, perpendicular to the y_2-axis and the angle between $\hat{c}$ and x_2-axis is less than $\pi/2$. The z-axis will follow the right-hand rule. The direction cosines of the unit vectors $\hat{p}_2$, $\hat{c}$, and $\hat{l}_3$ in the local coordinate system are expressed in the parenthesis for each unit vector as $\hat{p}_2$ (0, 1, 0), $\hat{c}$ (b_1, b_2, 0), and $\hat{l}_3$ (a_1, a_2, a_3), respectively.

The unknown direction cosines in the local coordinate system will be found by applying the dot product of unit vectors and using the known angles from its design. The direction cosine b_2 can be obtained from unit vectors $\hat{p}_2$ and $\hat{c}$ and the known angle γ as follows.

$$\hat{p}_2 \cdot \hat{c} = \hat{p}_{2x}\hat{c}_x + \hat{p}_{2y}\hat{c}_y + \hat{p}_{2z}\hat{c}_z \text{ in global coordinates}$$
$$= \cos\gamma$$
$$= b_2 \text{ in local coordinates} \tag{13}$$

from which

$$b_2 = \cos\gamma \tag{14}$$

where the angle γ between $\hat{p}_2$ and $\hat{c}$ is taken to be less than π. Therefore

$$b_1 = \sqrt{1 - b_2^2} = \sin\gamma \tag{15}$$

where the positive sign is taken for the square root as a result of construction of the local coordinate system.

The direction cosines a_1, a_2, and a_3 of unit vector $\hat{l}_3$ can be obtained as follows. From the dot product of $\hat{l}_3$ and $\hat{p}_2$, and $\hat{l}_3$ and $\hat{c}$ we have

$$-\hat{l}_3 \cdot \hat{p}_2 = -a_2 = \cos\alpha \tag{16}$$
$$-\hat{l}_3 \cdot \hat{c} = -a_1 b_1 - a_2 b_2 = \cos\delta \tag{17}$$

where the known angle α between $\hat{p}_2$ and $-\hat{l}_3$, and the unknown angle δ between $\hat{c}$ and $-\hat{l}_3$ are chosen to be less than π. By applying the cosine law to ΔABC

$$\cos\delta = (l_3^2 + c^2 - l_2^2)/2l_3 c \tag{18}$$

Therefore

$$a_1 = -(\cos\delta + a_2 b_2)/b_1 \tag{19}$$

in which b_1, b_2, a_2, and $\cos\delta$, have been just defined in equations (14)–(16), and (18). The direction cosine a_3 can now be calculated as

$$a_3 = \pm\sqrt{1 - a_1^2 - a_2^2} \tag{20}$$

The positive and negative signs of a_3 correspond to two possible positions of joint B for the given problem. If $1 - a_1^2 - a_2^2 = 0$, then the mechanism is not working.

Summarizing, we have

$$b_1 = \sin\gamma \quad a_1 = -(\cos\delta - \cos\alpha\cos\gamma)/\sin\gamma$$
$$b_2 = \cos\gamma \quad a_2 = -\cos\alpha$$
$$a_3 = \pm\sqrt{1 - a_1^2 - a_2^2} \tag{21}$$

The transformation matrix from local to global coordinates can now be determined as follows. As

$$\{\hat{p}_{2x}, \hat{p}_{2y}, \hat{p}_{2z}\}^T = [T_{ij}]_2 \quad \{0,1,0\}^T \tag{22}$$

and

$$\{\hat{c}_x, \hat{c}_y, \hat{c}_z\}^T = [T_{ij}]_2 \quad \{b_1, b_2, 0\}^T \tag{23}$$

from which

$$(T_{12})_2 = \hat{p}_{2x}, (T_{22})_2 = \hat{p}_{2y}, (T_{32})_2 = \hat{p}_{2z} \tag{24}$$

and

$$(T_{11})_2 = [\hat{c}_x - (T_{12})_2 b_2]/b_1$$
$$(T_{21})_2 = [\hat{c}_y - (T_{22})_2 b_2]/b_1 \tag{25}$$
$$(T_{31})_2 = [\hat{c}_z - (T_{32})_2 b_2]/b_1$$

Since each element in a direction cosine matrix is equal to its own cofactor, therefore

$$(T_{13})_2 = (T_{21})_2(T_{32})_2 - (T_{22})_2(T_{31})_2$$
$$(T_{23})_2 = (T_{12})_2(T_{31})_2 - (T_{11})_2(T_{32})_2 \tag{26}$$
$$(T_{33})_2 = (T_{11})_2(T_{22})_2 - (T_{12})_2(T_{21})_2$$

The resulting transformation matrix is

$$[T_{ij}]_2 = \frac{1}{\sin\gamma}\begin{bmatrix} \hat{c}_x - \hat{p}_{2x}\cos\gamma & \hat{p}_{2x}\sin\gamma & \hat{p}_{2z}\hat{c}_y - \hat{p}_{2y}\hat{c}_z \\ \hat{c}_y - \hat{p}_{2y}\cos\gamma & \hat{p}_{2y}\sin\gamma & \hat{p}_{2x}\hat{c}_z - \hat{p}_{2z}\hat{c}_x \\ \hat{c}_z - \hat{p}_{2z}\cos\gamma & \hat{p}_{2z}\sin\gamma & \hat{p}_{2y}\hat{c}_x - \hat{p}_{2x}\hat{c}_y \end{bmatrix} \tag{27}$$

Now the unit vector $\hat{l}_3$ in global coordinates can be obtained from

$$\{\hat{l}_{3x}, \hat{l}_{3y}, \hat{l}_{3z}\}^T = [T_{ij}]_2 \{a_1, a_2, a_3\}^T \tag{28}$$

and the vector $\bar{l}_3$ is

$$\bar{l}_3 = l_3 \hat{l}_3 \tag{29}$$

Note that

if $\alpha + \beta > \gamma$, l_3 has two positions

if $\alpha + \beta = \gamma$, l_3 has one position

if $\alpha + \beta < \gamma$, it is an impossible case

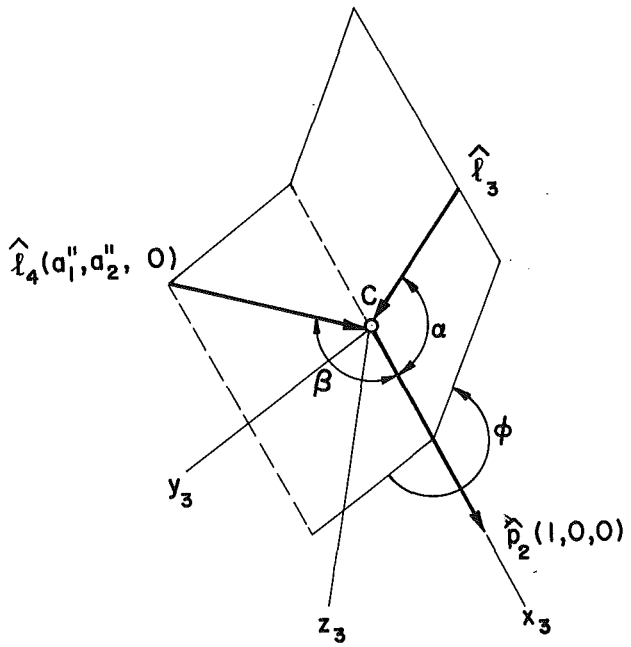

Fig. 5 A local coordinate system and output angle measurement

(*d*) **Analysis of $\hat{l}_2$.** Let us consider the equation

$$\bar{l}_2 + \bar{l}_3 + \bar{c} = 0 \tag{30}$$

or its scalar form

$$\begin{aligned} l_2\hat{l}_{2x} + l_3\hat{l}_{3x} + c\hat{c}_x &= 0 \\ l_2\hat{l}_{2y} + l_3\hat{l}_{3y} + c\hat{c}_y &= 0 \\ l_2\hat{l}_{2z} + l_3\hat{l}_{3z} + c\hat{c}_z &= 0 \end{aligned} \tag{31}$$

From these equations the components of unit vector $\hat{l}_2$ can be solved as

$$\begin{aligned} \hat{l}_{2x} &= -(l_3\hat{l}_{3x} + c\hat{c}_x)/l_2 \\ \hat{l}_{2y} &= -(l_3\hat{l}_{3y} + c\hat{c}_y)/l_2 \\ \hat{l}_{2z} &= -(l_3\hat{l}_{3z} + c\hat{c}_z)/l_2 \end{aligned} \tag{32}$$

Therefore

$$\bar{l}_2 = l_2\hat{l}_2 \tag{33}$$

(*e*) **Output Angle ϕ.** The output angle ϕ for the rotation about the $\hat{p}_2$-axis can be measured with any arbitrary reference. As shown in Fig. 5, ϕ is chosen as the angle between the two planes formed by $\hat{p}_2$ and $\hat{l}_4$, and $\hat{p}_2$ and $\hat{l}_3$, and $\hat{p}_2\hat{l}_4$ plane is chosen as a reference. Both the angle α between $\hat{p}_2$ and $-\hat{l}_3$ and the angle β between $\hat{p}_2$ and $-\hat{l}_4$ are chosen to be less than π and they are known angles from the mechanism.

Let the local coordinates x_3, y_3, and z_3 with the origin at C be chosen as follows:

x_3-axis is along the known rotating axis $\hat{p}_2$ and has the same positive direction as $\hat{p}_2$.

y_3-axis is in the plane of $\hat{p}_2$ and $\hat{l}_4$ and the angle between $-\hat{l}_4$ and the y-axis is less than $\pi/2$.

z_3-axis follows the right-hand rule.

It is seen that the angle ϕ can now be measured between x_3y_3-plane and x_3l_3-plane with x_3y_3-plane as reference.

The direction cosines of the unit vectors $\hat{p}_2$, $\hat{l}_3$, and $\hat{l}_4$ in the local coordinate system are expressed in the parenthesis for each unit vector as $\hat{p}_2$ (1, 0, 0), $\hat{l}_3$ ($-\cos\alpha$, $-\sin\alpha\cos\phi$, $-\sin\alpha\sin\phi$), and (a_1'', a_2'', 0), respectively.

To find ϕ, the same procedure used to find $\hat{l}_1$ will be followed. The transformation matrix $[T_{ij}]_3$ is obtained as

$$[T_{ij}]_3 = \frac{1}{\sin\beta}\begin{bmatrix} \hat{p}_{2x}\sin\beta & -\hat{l}_{4x} - \hat{p}_{2x}\cos\beta & -\hat{p}_{2y}\hat{l}_{4z} + \hat{p}_{2z}\hat{l}_{4y} \\ \hat{p}_{2y}\sin\beta & -\hat{l}_{4y} - \hat{p}_{2y}\cos\beta & -\hat{p}_{2z}\hat{l}_{4x} + \hat{p}_{2x}\hat{l}_{4z} \\ \hat{p}_{2z}\sin\beta & -\hat{l}_{4z} - \hat{p}_{2z}\cos\beta & -\hat{p}_{2x}\hat{l}_{4y} + \hat{p}_{2y}\hat{l}_{4x} \end{bmatrix} \tag{34}$$

Therefore

$$\{\hat{l}_{3x}, \hat{l}_{3y}, \hat{l}_{3z}\}^T = -[T_{ij}]_3\{\cos\alpha, \sin\alpha\cos\phi, \sin\alpha\sin\phi\}^T \tag{35}$$

This equation in $\hat{l}_3$ can be expanded into

$$\begin{aligned} \hat{l}_{3x} &= -[(T_{11})_3\cos\alpha + (T_{12})_3\sin\alpha\cos\phi + (T_{13})_3\sin\alpha\sin\phi] \\ \hat{l}_{3y} &= -[(T_{21})_3\cos\alpha + (T_{22})_3\sin\alpha\cos\phi + (T_{23})_3\sin\alpha\sin\phi] \\ \hat{l}_{3z} &= -[(T_{31})_3\cos\alpha + (T_{32})_3\sin\alpha\cos\phi + (T_{33})_3\sin\alpha\sin\phi] \end{aligned} \tag{36}$$

From any two of these three equations $\sin\phi$ and $\cos\phi$ can be solved. If the first two equations are chosen, we obtain

$$\sin\phi = \frac{[-(T_{22})_3\hat{l}_{3x} + (T_{12})_3\hat{l}_{3y}] - [(T_{11})_3(T_{22})_3 - (T_{12})_3(T_{21})_3]\cos\alpha}{[(T_{13})_3(T_{22})_3 - (T_{12})_3(T_{23})_3]\sin\alpha} \tag{37}$$

$$\cos\phi = \frac{[-(T_{23})_3\hat{l}_{3x} - (T_{13})_3\hat{l}_{3y}] - [(T_{11})_3(T_{23})_3 - (T_{13})_3(T_{21})_3]\cos\alpha}{[(T_{12})_3(T_{23})_3 - (T_{13})_3(T_{22})_3]\sin\alpha} \tag{38}$$

These two equations can be simplified as

$$\sin\phi = \frac{(T_{22})_3\hat{l}_{3x} - (T_{12})_3\hat{l}_{3y} + (T_{33})_3\cos\alpha}{(T_{31})_3\sin\alpha} \tag{39}$$

$$\cos\phi = \frac{-(T_{23})_3\hat{l}_{3x} + (T_{13})_3\hat{l}_{3y} + (T_{32})_3\cos\alpha}{(T_{31})_3\sin\alpha} \tag{40}$$

From these two equations the angle ϕ can be completely determined.

2 Displacement Analysis of the RGCR Mechanism

The RGCR four-link spatial mechanism whose schematic diagram is shown in Fig. 6 is similar to the RGGR mechanism except that one of the spherical joints is replaced by a cylindrical joint.

The known data of the mechanism for the analysis are the lengths l_1, l_2, the vector $\bar{l}_4$, the directions of rotation of $\hat{p}_1$, $\hat{p}_2$, the angles ζ, η, α, β, and the input angle θ. The unknown quantities are $\hat{l}_1$, l_2, and $\hat{l}_3$. The angles, ζ between $\hat{p}_1$ and $\hat{l}_1$, η between $\hat{p}_1$ and $\hat{l}_4$, α between $\hat{p}_2$ and $\hat{l}_3$, and β between $\hat{p}_2$ and $\hat{l}_4$ are chosen to be less than π and they are known angles from the construction of the mechanism.

In the analysis, the only difference from the RGGR is the calculation of $\bar{l}_3$. The analysis of $\hat{l}_3$ is as follows. From Fig. 6,

$$\bar{c} = \bar{l}_1 - \bar{l}_4 \quad \text{and} \quad \hat{c} = \bar{c}/|\bar{c}| \tag{41}$$

By applying cosine law to ΔABC we obtain

$$c^2 = l_2^2 + l_3^2 - 2l_2l_3\cos\psi \tag{42}$$

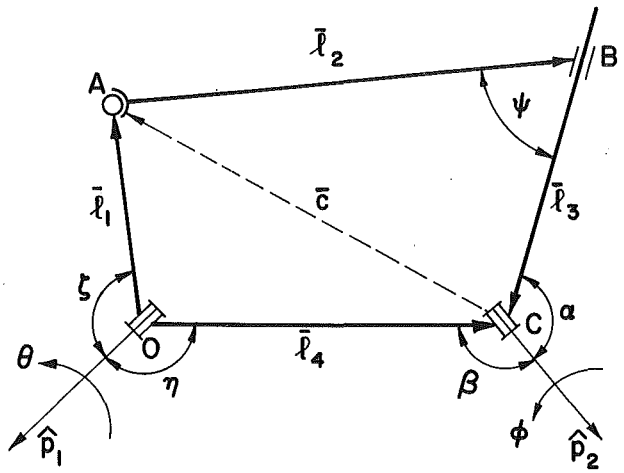

Fig. 6 The schematic diagram of a RGGR four-line spatial mechanism and its known data

To solve l_3 the preceding equation is rewritten as

$$l_3^2 - (2l_2\cos\psi)l_3 + (l_2^2 - c^2) = 0 \tag{43}$$

This gives

$$l_3 = l_2\cos\psi \pm \sqrt{c^2 - l_2^2\sin^2\psi} \tag{44}$$

in which the rules of choice of positive and negative signs before the square root are as follows:

(*i*) For $\psi \geq \pi/2$ positive sign only and there is only one solution.

(*ii*) For $\psi < \pi/2$ and $\sqrt{c^2 - l^2\sin^2\psi} > l_2\cos\psi$, positive sign only and there is only one solution.

(*iii*) For $\psi < \pi/2$ and $l_2\cos\psi > \sqrt{c^2 - l^2\sin\psi}$, positive and negative signs correspond to two positions for two solutions of l_3.

Figure 7 illustrates the choice of these rules. Also by applying the cosine law to ΔABC, we obtain

$$\cos\delta = (l_3^2 + c^2 - l_2^2)/2l_3c. \tag{45}$$

Now, the unknown unit vectors $\hat{l}_3$ can be obtained in the same manner as finding $\hat{l}_3$ in the RGGR mechanism by using the local coordinate system and their direction cosines of corresponding unit vectors.

3 Displacement Analysis of the RRGG Mechanism

The RRGG four-link spatial mechanism is a variation of the popular RGGR four-link spatial linkage. Each mechanism has a single degree of freedom, with a passive degree of freedom in the GG link. A schematic diagram of a RRGG mechanism is shown in Fig. 8.

The known quantities of the mechanism are the lengths l_1, l_2, and l_3, the vector $\bar{l}_4$, the direction of rotation $\hat{p}_1$, the angles ζ, η, α, and β from the linkage design, and the input angle θ. The angle ζ, between $\hat{p}_1$ and $\hat{l}_1$, and the angle η, between $\hat{p}_1$ and $\hat{l}_4$, are chosen to be less than π.

Both the angle α, between $\hat{p}_2$ and $\hat{l}_2$, and the angle β, between $\hat{p}_2$ and $-\hat{l}_1$, are also chosen to be less than π. The unknown quantities are $\hat{l}_1$, $\hat{l}_2$, and $\hat{l}_3$.

After calculating $\hat{l}_1$ by equation (11), $\hat{p}_2$ is determined by the direction cosine matrix method as illustrated earlier. $\hat{p}_2$ is calculated as

$$\begin{Bmatrix} \hat{p}_{2x} \\ \hat{p}_{2y} \\ \hat{p}_{2z} \end{Bmatrix} = \frac{1}{\sin\zeta} \begin{bmatrix} \hat{p}_{1x} + \hat{l}_{1x}\cos\zeta & -\hat{l}_{1x}\sin\zeta & \hat{l}_{1y}\hat{p}_{1z} - \hat{l}_{1z}\hat{p}_{1y} \\ \hat{p}_{1y} + \hat{l}_{1y}\cos\zeta & -\hat{l}_{1y}\sin\zeta & \hat{l}_{1z}\hat{p}_{1x} - \hat{l}_{1x}\hat{p}_{1z} \\ \hat{p}_{1z} + \hat{l}_{1z}\cos\zeta & -\hat{l}_{1z}\sin\zeta & \hat{l}_{1x}\hat{p}_{1y} - \hat{l}_{1y}\hat{p}_{1x} \end{bmatrix} \begin{Bmatrix} b_1 \\ b_2 \\ b_3 \end{Bmatrix} \tag{46}$$

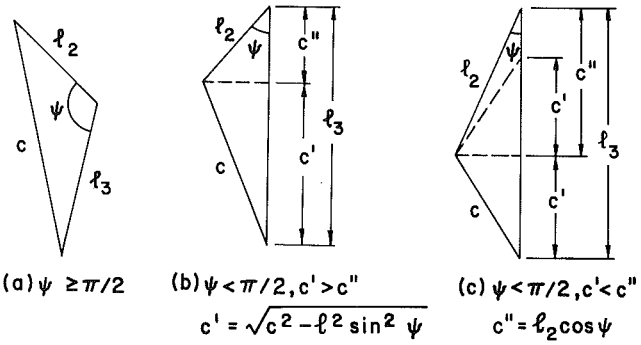

Fig. 7 Transmission angle and l_3

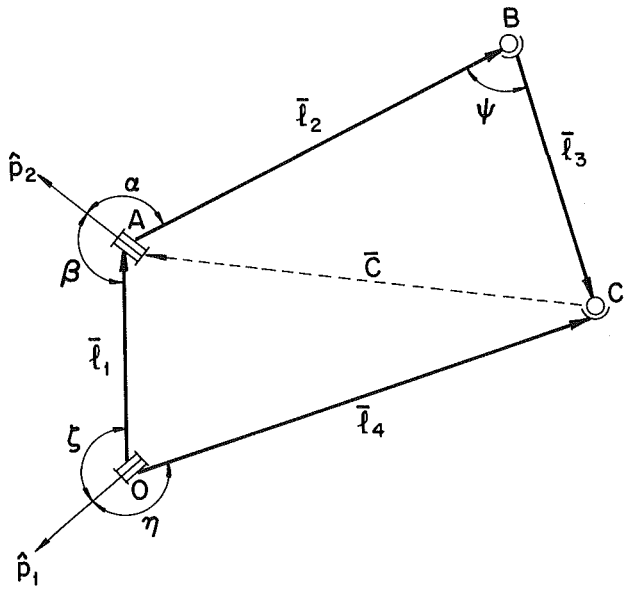

Fig. 8 The schematic diagram of the RRGG mechanism and its known data

where

$$b_1 = (\cos\rho - \cos\zeta\cos\beta)/\sin\zeta$$
$$b_2 = \cos\beta$$
$$b_3 = \pm\sqrt{1 - b_1^2 - b_2^2}$$

The positive and negative signs of b_3 can be decided from the observation of the given mechanism construction in the local coordinate system.

Once $\hat{p}_2$ is determined, the analyses of $\hat{l}_2$ and $\hat{l}_3$ of the RRGG are similar procedure as the analysis of $\hat{l}_2$ and $\hat{l}_3$ of the RGGR by letting $\hat{l}_2$ and $\hat{l}_3$. Therefore, the transformation matrix equation (27) could be used with negative $\hat{c}$ components in calculation of $\hat{l}_2$.

The output angle ϕ for the rotation about the $\hat{p}_2$-axis can be measured with any arbitrary reference. The ouptut angle ϕ is chosen as the angle between the two planes formed by $\hat{p}_2$ and $\hat{l}_1$, and $\hat{p}_2$ and $\hat{l}_2$. The p_2l_2-plane is chosen as a reference. The output angle could be completely determined from the following two equations

$$\sin\phi = \frac{-(T_{22})_4\hat{l}_{2x} + (T_{12})_4\hat{l}_{2y} + (T_{33})_4\cos\alpha}{(T_{31})_4\sin\alpha} \tag{47}$$

and

$$\cos\phi = \frac{(T_{23})_4 \hat{l}_{2x} - (T_{13})_4 \hat{l}_{2y} + (T_{32})_4 \cos\alpha}{(T_{31})_4 \sin\alpha} \tag{48}$$

where the transformation matrix $[T_{ij}]_4$ is obtained as

$$[T_{ij}]_4 = \frac{1}{\sin\beta} \begin{bmatrix} \hat{p}_{2x}\sin\beta & -\hat{l}_{1x} - \hat{p}_{2x}\cos\beta & -\hat{p}_{2y}\hat{l}_{1z} + \hat{p}_{2z}\hat{l}_{1y} \\ \hat{p}_{2y}\sin\beta & -\hat{l}_{1y} - \hat{p}_{2y}\cos\beta & -\hat{p}_{2z}\hat{l}_{1x} + \hat{p}_{2x}\hat{l}_{1z} \\ \hat{p}_{2z}\sin\beta & -\hat{l}_{1z} - \hat{p}_{2z}\cos\beta & -\hat{p}_{2x}\hat{l}_{1y} + \hat{p}_{2y}\hat{l}_{1x} \end{bmatrix} \tag{49}$$

4 Displacement Analysis of the RRGC Mechanism

The displacement analysis of the RRGC four-link spatial mechanism shown in Fig. 9 can be performed by using part of the analysis scheme of the RRGG.

The known data of the RRGC mechanism shown in Fig. 9 are the lengths l_1 and l_2, the vectors $\bar{l}_4$, and $\hat{l}_3$, the direction of rotation $\hat{p}_1$, the angles ζ, η, α, β, ϵ, and the input angle θ. The definition of the angles is the same as the RRGG, except angle ϵ between $\hat{l}_3$ and $\hat{l}_4$, which is chosen to be less than π. The unknown quantities of this mechanism are $\hat{l}_1$, $\hat{l}_2$, and l_3.

The displacement analysis of the RRGC can be performed easily by using part of the analysis scheme of the RRGG for $\hat{p}_2$ and part of the similar analysis scheme of the RGCR for l_3 and the output angle.

5 Numerical Examples

For the numerical illustrations, the dimensions and other known data of the spatial four-bar linkages are given as follows.

Example 1

RGGR mechanism

l_1 = 101.6 mm
l_2 = 381.0 mm
l_3 = 254.0 mm
l_4 = 314.2 mm
$\bar{l}_4$ = (304.8, 0, 76.2)
$\hat{p}_1$ = (0, 0, 1)
$\hat{p}_2$ = (1, 0, 0)
ρ = 90 deg
α = 90 deg

Example 2

RGCR mechanism

l_1 = 203.2 mm
l_2 = 381.0 mm
l_4 = 314.2 mm
$\bar{l}_4$ = (304.8, 0, 76.2)
$\hat{p}_1$ = (0, 0, 1)
$\hat{p}_2$ = (0, 0, 1)
ρ = 90 deg
α = 90 deg
ψ = 74 deg

Example 3

RRGG mechanism

l_1 = 119.0 mm
l_2 = 248.6 mm
l_3 = 186.7 mm
l_4 = 225.6 mm
$\hat{l}_4$ = (1, 0, 0)
$\hat{p}_1$ = (0, 0, 1)
α = 90 deg
β = 92.27 deg
γ = 0 deg
ρ = 158.17 deg

Example 4

RRGC mechanism

l_1 = 119.0 mm
l_2 = 248.6 mm
l_4 = 228.6 mm
$\hat{l}_3$ = (0.4082, 0.8165, 04082)
$\hat{l}_4$ = (1, 0, 0)
$\hat{p}_1$ = (0, 0, 1)
ζ = 90 deg
α = 90 deg
ϵ = 108 deg

With input angle θ as a parameter, the vectors $\bar{l}_1$, $\bar{l}_2$, and $\bar{l}_3$, the output angle ϕ, and the transmission angle ψ are determined. The transmission angle is defined as an angle between $-\hat{l}_2$ and $\hat{l}_3$. The results of Example 1 are tabulated in Table 1 for two possible configurations of the RGGR mechanism, i.e., there are two output angles ϕ_1 and ϕ_2 for a given input angle θ. The transmission angles are the same in both configurations. Table 2 shows three components of each of the vector $\bar{l}_1$, $\bar{l}_2$, and $\bar{l}_3$ in the global coordinates corresponding to a particular input angle, in this case, θ = 60 deg for the RGGR mechanism. For Example 2, Table 3 shows output angle and the calculated length of link 3 corresponding to input angle θ in the RGGR mechanism.

For Examples 3 and 4, the results are tabulated in Table 4 for the RRGG mechanism and in Table 5 for the RRGC mechanism. Tables 4 and 5 show the results of the transmission angle and output angle for each input angle.

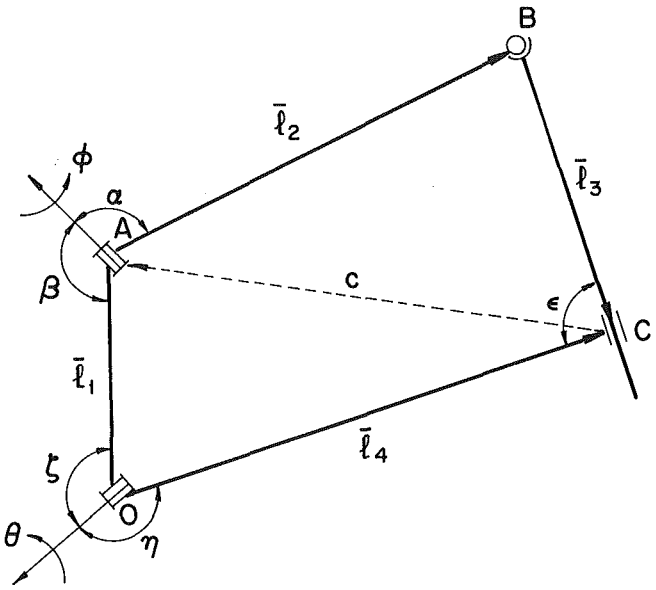

Fig. 9 The schematic diagram of RRGC four-link spatial mechanism and its known data

Table 1 Output angle ϕ and transmission angle ψ versus input angle θ of the RGGR mechanism, all angles in degree

θ	ϕ_1	ϕ_2	ψ
110	91.6	165.6	65.8
100	75.1	179.5	62.3
90	63.0	190.8	58.7
80	53.3	201.3	54.9
70	45.3	211.9	51.0
60	38.4	223.4	47.2
50	32.5	236.3	43.5
40	27.4	251.4	40.1
30	23.4	269.2	37.1
20	21.0	290.0	34.8
10	21.8	312.1	33.4
0	29.9	330.1	32.9
−10	47.9	338.2	33.4
−20	70.0	339.0	34.8
−30	90.8	336.6	37.1
−40	108.6	332.6	40.1
−50	123.7	327.5	43.5
−60	136.6	321.6	47.2
−70	148.1	314.7	51.0
−80	158.7	306.7	54.9
−90	169.2	297.0	58.7
−100	180.5	284.9	62.3
−110	194.4	268.4	65.8

Table 2 Positions of the RGGR mechanism in system coordinates at θ = 60 deg, all lengths in mm

	Configuration 1			Configuration 2			
	$\hat{i}$	$\hat{j}$	$\hat{k}$	$\hat{i}$	$\hat{j}$	$\hat{k}$	Resultant
$\bar{l}_1$	50.8	88.0	0.0	50.8	88.0	0.0	101.6
$\bar{l}_2$	254.0	69.8	275.3	254.0	−262.5	−108.4	381.0
$\bar{l}_3$	0.0	−157.2	−199.1	0.0	174.5	184.6	254.0
$\bar{l}_4$	304.8	0.0	76.2	304.8	0.0	76.2	314.2

Table 3 Output angle ϕ and the length of link 3 versus input angle θ of the RGCR mechanism, angles in degree and lengths in mm

θ	ϕ_1	l_3
90	248.4	181.6
100	264.3	270.5
110	274.5	324.6
120	282.6	365.4
130	289.5	397.4
140	295.7	422.5
150	301.3	441.4
160	306.3	454.7
170	311.0	462.6
180	315.2	465.2
190	318.9	462.6
200	322.3	454.7
210	325.1	441.4
220	327.4	422.5
230	328.9	397.4
240	329.4	365.4
250	328.5	324.6
260	325.1	270.5
270	315.8	181.6

In the numerical example of configuration 2 of the RRGC mechanism, the input angle is limited to the range of 80 to -160 deg due to the construction of the mechanism. Another limitation should be observed. The motion that joint B of the mechanism passes through the cylindrical joint C during an increment of the input angle from -100 to -110 deg is impossible in actual cases, although it is theoretically possible in the analysis. Therefore, the range of motion of configuration 2 is divided into two intervals -80 to -100 deg and -110 to -160 deg.

Conclusion

The direction cosine matrix method has been developed for a displacement analysis applicable to all types of four-link, spatial mechanisms. The analyses of the RGGR, RGCR, RRGG, and RRGC mechanisms have been illustrated to demonstrate this method. The advantage of this method is that the analysis yields exact solutions without loss of geometric interpretation and without the need for either numerical or iterative schemes.

The special property of the direction cosine matrix, that each element equals its own cofactor, is the focus of this analysis. Using this property, we avoid the inherent difficulties in the displacement analysis of four-link spatial mechanisms. For example, without using this property, equation (9) would be replaced by

$$T_{13} = \pm\sqrt{1 - T_{11}^2 - T_{12}^2}$$

$$T_{23} = \pm\sqrt{1 - T_{21}^2 - T_{22}^2}$$

$$T_{33} = \pm\sqrt{1 - T_{31}^2 - T_{32}^2}$$

and only one of the eight sets of possible combinations would be the solution. In another example, an algebraic equation of up to eighth-degree polynomial in reference [10] has to be solved numerically.

The extension of this method to a displacement analysis of mechanisms with more than four links and the continuation of kinematic analyses for determining velocities and accelerations of mechanisms with four or more links will be the topics of forthcoming papers.

Table 4 Output angle ϕ and transmission angle ψ versus input angle θ of the RRGG mechanism, all angles in degree

θ	ϕ_1	ϕ_2	ψ
0	137.5	225.8	24.2
10	156.0	245.4	25.4
20	172.9	263.6	28.8
30	188.3	279.5	33.6
40	202.3	293.1	39.2
50	215.1	304.6	45.4
60	227.1	314.3	51.8
70	238.3	322.8	58.3
80	248.7	330.3	64.7
90	258.6	337.1	71.0
100	268.0	343.4	77.1
110	276.8	349.3	82.8
120	285.1	355.0	33.2
130	293.0	0.6	93.0
140	300.5	6.1	97.1
150	307.6	11.6	100.5
160	374.3	17.3	103.0
170	320.8	23.1	104.6
180	326.9	29.1	105.1
190	332.9	35.4	104.6
200	338.6	41.9	103.0
210	344.2	48.8	100.5
220	349.8	56.0	97.1
230	355.3	63.6	93.0
240	0.9	71.7	88.2
250	6.8	80.1	82.8
260	12.9	89.1	77.1
270	19.4	98.6	71.0
280	26.6	108.6	64.7
290	34.7	119.4	58.3
300	43.9	130.9	51.8
310	54.6	143.3	45.4
320	67.2	156.8	39.2
330	82.1	171.7	33.6
340	99.3	188.1	28.8
350	118.1	206.4	25.4
360	137.5	225.8	24.2

Table 5 Output angle ϕ and transmission angle ψ versus input angle θ of the RRGC mechanism, all angles in degree

θ	ϕ_1	ψ_1	ϕ_2	ψ_2
Interval 1				
80	293.5	79.1	276.2	100.9
70	297.1	65.3	258.2	114.7
60	297.0	55.8	242.3	124.2
50	295.3	47.6	225.8	132.4
40	292.5	40.2	208.0	139.8
30	288.7	33.6	189.2	146.4
20	283.8	27.9	170.5	152.1
10	277.8	23.2	153.3	156.8
0	270.8	19.8	138.3	160.2
−10	262.5	17.8	125.4	162.2
−20	252.8	17.0	114.4	163.0
−30	241.3	17.3	104.9	162.7
−40	227.7	18.3	96.5	161.7
−50	212.0	20.0	89.0	160.0
−60	194.9	22.3	82.3	157.7
−70	177.3	25.1	76.1	155.0
−80	160.8	28.3	70.3	151.7
−90	145.9	32.0	64.8	148.0
−100	132.7	36.1	59.6	143.9
Interval 2				
−110	120.8	40.8	54.7	139.2
−120	109.7	45.9	49.9	134.1
−130	98.9	51.7	45.3	128.3
−140	87.8	58.2	41.2	121.8
−150	75.5	66.0	37.9	114.0
−160	59.7	76.7	37.2	103.3

References

1 Yang, A. T., "A Brief Survey of Space Mechanisms," *Design Technology Transfer*, ASME, 1974, pp. 315-321.

2 Uicker, J. J., Jr., "Displacement Analysis of Spatial Mechanisms by an Iterative Method Based on 4×4 Matrices," M.S. thesis, Northwestern University, Evanston, Ill., June, 1963.

3 Uicker, J. J., Jr., Denavit, J., and Hartenberg, R. S., "An Iterative Method for the Displacement Analysis of Spatial Mechanisms," ASME JOURNAL OF APPLIED MECHANICS, Vol. 31, 1964, pp. 309–314.

4 Yang, A. T., "Application of Quaternion Algebra and Dual Numbers to the Analysis of Spatial Mechanisms," Ph. D. Dissertation, Columbia University, New York, 1963.

5 Yang, A. T., and Freudenstein, F. F., "Application of Dual-Number Quaternion Algebra to the Analysis of Spatial Mechanism," ASME JOURNAL OF APPLIED MECHANICS, Vol. 31, 1964, pp. 300–308.

6 Gupta, V. K., "Kinematic Analysis of Plane and Spatial Mechanisms," ASME *Journal of Engineering for Industry*, Vol. 95, 1973, pp. 481–486.

7 Suh, Chung-Ha, and Radcliffe, C. W., *Kinematics and Mechanisms Design*, Wiley, New York, 1978, pp. 79–94.

8 Chace, M., "Vector Analysis of Linkages," ASME *Journal of Engineering for Industry*, Vol. 85, 1963, pp. 289–297.

9 Chace, M., "Development and Application of Vector Mathematics for Kinematic Analysis of Three-Dimensional Mechanisms," Ph.D. Dissertation, University of Michigan, Ann Arbor, Mich., 1964.

10 Chace, M., "Solutions to the Vector Tetrahedron Equations," ASME *Journal of Engineering for Industry*, Vol. 87, 1965, pp. 228–234.

11 Dimentberg, F. M., *The Determination of the Positions of Spatial Mechanism*, Akad Nauk., Moscow, USSR, 1950, p. 142.

12 Dimentberg, F. M., and Kislitsyn, S. G., "Application of Screw Calculus to the Analysis of Three-Dimensional Mechanisms," *Proceedings of the Second All-Union Conference on Basic Problems in the Theory of Machines and Mechanisms*, Moscow, USSR, 1960, pp. 55–56.

13 Soni, A. H., and Harrisberger, L., "Application of (3 × 3) Screw Matrix to Kinematic and Dynamic Analysis of Mechanisms," *VD1-Brichte*, 1968.

14 Bagci, C., "The RSRC Space Mechanism Analysis by 3 × 3 Screw Matrix, Synthesis for Screw Generation by Variational Methods," Dissertation, Oklahoma State University, Stillwater, Okla., 1969.

15 Duffy, J., "An Analysis of Five, Six and Seven-Link Spatial Mechanisms," *Proceedings of Third World Congress for the Theory of Machines and Mechanisms*, Kupari, Yugoslavia, 1971, Vol. C, pp. 83–98.

16 Ho, C. Y., "An Analysis of Spatial Four-Bar Linkage by Tensor Method," *IBM Journal of Research and Development*, Vol. 10, No. 3, May 1966, pp. 207–212.

17 Yuan, M. S. C., "Displacement Analysis of the RRCCR Five-Link Spatial Mechanism," ASME JOURNAL OF APPLIED MECHANICS, Vol. 37, 1970, pp. 689–696.

18 Wallace, D. M., and Freudenstein, F. F., "The Displacement Analysis of the Generalized Tracta Coupling," ASME JOURNAL OF APPLIED MECHANICS, Vol. 37, 1970, pp. 713–718.

19 Harrisberger, L., "A Number Synthesis Survey of Three-Dimensional Mechanisms," ASME *Journal of Engineering for Industry*, Vol. 87, 1965, pp. 213–220.

20 Hartenberg, R. S., and Denavit, J., *Kinematic Synthesis of Linkages*, McGraw-Hill, New York, 1964, pp. 344–347.